JMEPEG (2012) 21:2038–2043
DOI: 10.1007/s11665-012-0137-z

1059-9495/$19.00

Numerical Investigation into Effective Elastic Constants of MHS/EP Composite

Wei Yu, Meijuan Xin, Xi Liang, and Huijian Li

(Submitted June 4, 2011; in revised form December 9, 2011)

The metallic hollow sphere (MHS) periodically filled in epoxy is a type of syntactic metallic hollow sphere structure (MHS/EP). In this article, the effective elastic constants of MHS/EP composite with three kinds of packing types of MHS are numerically investigated by ANSYS. The unit cell is used to simplify MHS periodically filled composite, and the effective elastic moduli and Poisson's ratios are analyzed. It is found that the composite for simple cubic packing type can be considered as orthogonal isotropic material. However, the composites for the other two kinds of packing types should be considered as orthotropic materials in most instances, but they can be considered as orthogonal isotropic materials in relation to their linear-elastic behavior when the shell is medium-thickness wall.

Keywords effective elastic constants, metallic hollow sphere (MHS), periodically filled composite

1. Introduction

Cellular metallic materials such as honeycombs and metal foams are characterized by super-light, high specific stiffness and strength, the energy-absorbing capacity in the plastic deformation. It has been widely used for many applications such as automobile, aircraft, civil ,and military (Ref 1, 2). However, conventional cellular metallic materials like foamed aluminum have large varieties in the size, shape, and distribution of cells. It is difficult to monitor their mechanical properties. Metallic hollow sphere (MHS) structure composed by a group of small MHS is a new type of cellular metallic materials with easily reproducible geometry and consistent mechanical properties. In recent years, many studies on MHS have been done. Sanders and Gibson (Ref 3) analyzed the elastic moduli and the initial yield strength of body-centered cubic and face-centered cubic packings of hollow sphere foams, and found that the FCC packing gives the highest values of moduli and strengths. Based on the experimental study of the behavior of random hollow sphere metal foam, Lim et al. (Ref 4) found that its unloading stiffness and plastic collapse stress seem more consistent with open-cell foams. Gasser et al. (Ref 5) studied the uniaxial tensile elastic properties of regular stacking of brazed hollow spheres, and a model derived from thin shell elastic properties was proposed. Then, Gasser et al. (Ref 6) numerically investigated the elastic properties of regular FCC stacking of hollow spheres. A slightly elastic anisotropy of the material and a negative Poisson's ratio was found. Fiedler et al. (Ref 7-9) mentioned two types of MHS structures, i.e., partially bonded MHSS and syntactic MHSS. They studied the thermal conductivity and mechanical properties of adhesively bonded MHS structure, and a quasi-isotropic, in relation to their linear-elastic behavior and uniaxial initial yield stresses of MHS structure with a primitive cubic arrangement was found. The thermal conductivity of MHSS was analyzed using analytical models by Solórzano et al. (Ref 10). The main structural parameters (sphere diameter, shell thickness, and constituent metal) were considered. Feyel and Marcadon (Ref 11) dedicated to the study of the mechanical behavior of MHSS under quasi-static compressive loads and to the characterization of contributions of both the stacking pattern and the constitutive material's mechanical properties. The quasi-static mechanical behavior of hollow stainless steel sphere foam was studied with static x-ray tomography by Lhuissier et al. (Ref 12). The size effects and damage mechanisms at the mesoscale were investigated. Friedl et al. (Ref 13) investigated the mechanical behavior of MHS structures under quasi-static compression experimentally.

Ruan et al. (Ref 14) studied the plastic crushing behavior of thin-walled spheres and sphere arrays experimentally. Selecting ping pong balls as the hollow spheres, a number of bifurcation phenomena were identified, and the effects of their crushing forces were illustrated. Karagiozova et al. (Ref 15) proposed a model of MHS cellular solid in large strain, and found that the proposed structural approach gives an adequate description of the deformation of MHS cellular solids in relatively large strains. Gao et al. (Ref 16) studied the mechanical properties of MHS materials during their large plastic deformation by finite element simulations, and the empirical functions of the relative material density were proposed for the elastic modulus, yield strength, and plateau stress for FCC packing. Dong et al. (Ref 17) studied the dynamic behavior of thin-walled spheres and sphere arrays by using SHPB test system. Ping pong balls were selected to study the collapse of the thin-walled spheres. It is found that the deformation of thin-walled elastic spherical shell depends on the impact of velocity. The effect of strain rate on the shell material is important in the analysis of the shell's response to dynamic loading. The high strain rate compression

Wei Yu, Xi Liang, and **Huijian Li**, Key Laboratory of Mechanical Reliability for Heavy Equipments and Large Structures of Hebei Province, Yanshan University, Qinhuangdao 066004, China; and **Meijuan Xin**, China Academy of Aerospace Aerodynamics, Beijing 100074, China. Contact e-mail: ysulhj@163.com.

deformation of stainless steel MHS was determined both numerically and experimentally by Tasdemirci et al. (Ref 18). They found that the contribution of the cell wall material rate, which is sensitive to the increased stress values at high strain rate, is higher than that of inertial effects on MHS structure investigated within the studied strain rate limits. Motz et al. (Ref 19) studied on fatigue crack propagation in MHSS. They measured a ratio of the fatigue strength divided by the yield stress in the range of 0.5-0.65 in compression and in the range of 0.2-0.25 in tension. Caty et al. (Ref 20) recently studied on fatigue of MHSS. An experimental determination of the fatigue properties with a large range of MHSS was provided. It is found that the constitutive material and the density are the two parameters that have the most important effect on the fatigue strength.

The MHS-resin composite was mentioned in the literature (Ref 7, 21). The MHS/EP composite is a type of syntactic MHS structure. However, wall thickness effect and elastic constants of MHS/EP composite with different filling types are seldom reported. In this article, the effective elastic moduli and Poison's ratios of three types of MHS/EP composites are numerically investigated.

2. Numerical Simulation

For the MHS/EP, the MHS is the main body frame, and the EP serves as a filler. The MHS's diameter is 23 mm, and the

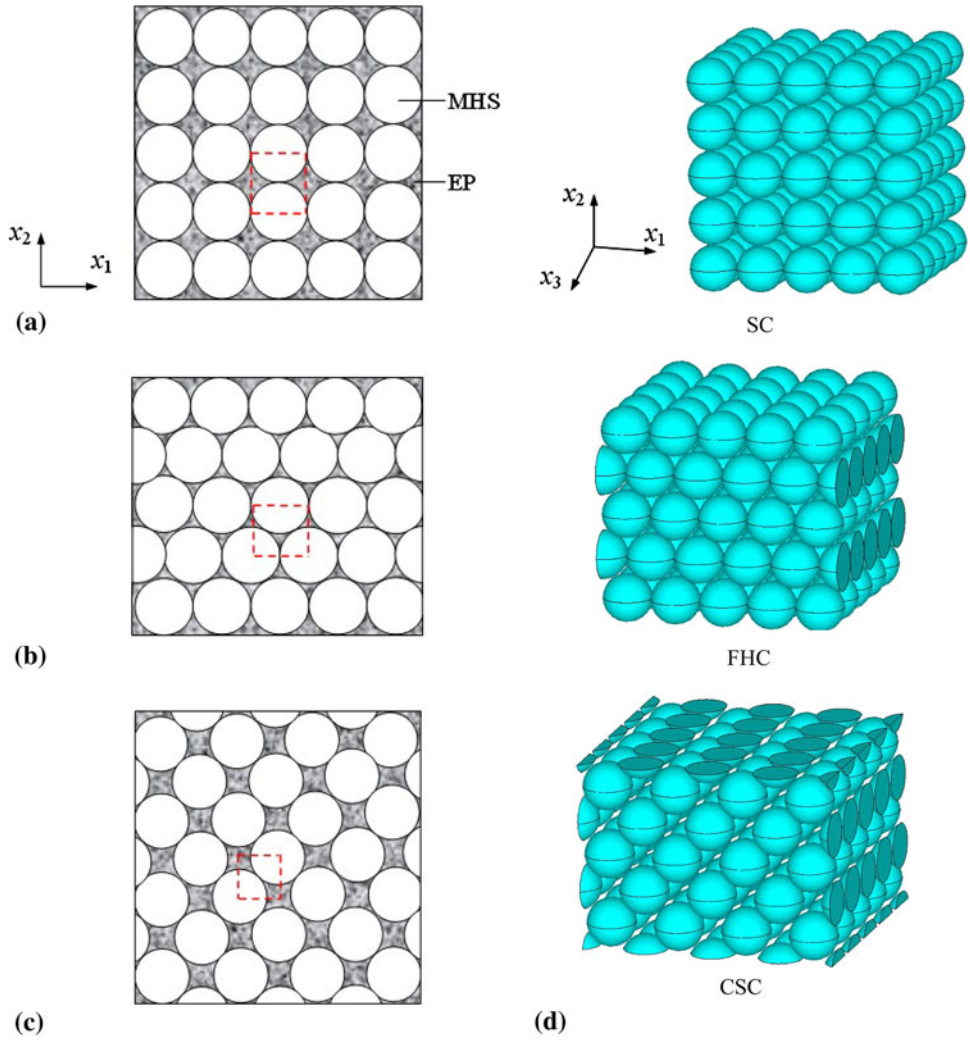

Fig. 1 Cross sections perpendicular to x_3 and their 3D plots. (a) Simple cubic packing, SC, (b) face-hexagonal cubic packing, FHC, (c) cater-cornered simple cubic packing, CSC, and (d) 3D plots of MHS

Table 1 The parameter of unit cell

	SC			FHC			CSC		
Packing types	x_1	x_2	x_3	x_1	x_2	x_3	x_1	x_2	x_3
Length of side of unit cell, mm	11.5	11.5	11.5	11.5	20	11.5	16.3	16.3	11.5
Number of elements	31,595			36,947			67,449		

modulus of constituent material is 46 GPa. The modulus and Poisson's ratio of EP are 3.6 GPa and 0.38, respectively. In this simulation, four types of thickness of MHS, i.e., $t = 0.1$, 0.2, 0.5, and 1.0 mm, and three types of packing types of MHS are considered. Figure 1 shows the cross section perpendicular to direction x_3. If the material size is far greater than MHS's diameter, then the packing volume ratios of MHS for these three types of composites are $\phi_{SC} = 52.33\%$, $\phi_{FHC} = 60.18\%$ and $\phi_{CSC} = 52.33\%$ respectively.

If MHSs are periodically distributed in epoxy matrix, then the entire material model is an infinite heterogeneous body with periodic change. The elastic matrix $[C]$ and flexibility matrix $[S]$ are a function of position x_1, x_2, and x_3. Therefore, the inner stress fields of composites are distributed periodically under symmetrical load. Accordingly, unit cell method is used to simplify MHS periodically filled composite model, where, the unit cell of simple cubic (SC) is one-eighth of the dashed frame area in Fig. 1(a), the unit cell of FHC is one fourth of it in Fig. 1(b), and the unit cell of CSC is one-half of it in Fig. 1(c). Table 1 shows the parameters of unit cells. The element of EP is solid 95, and the element of MHS is shell 63. The unit cells and their meshing are shown in Fig. 2. The displacement loading method is adopted, and the maximum displacement is 0.1 mm.

For the entire composite, the periodicity can be expressed as

$$\sigma(x_i + nd_i) = \sigma(x_i),\ \varepsilon(x_i + nd_i) = \varepsilon(x_i),\ C(x_i + nd_i) = C(x_i) \quad \text{(Eq 1)}$$

where, d_i is the edge vector of the unit cell.

Boundary conditions of unit cell must make it to satisfy the continuous and periodic conditions. Therefore, boundary conditions should be set as follows: restraining the rotations of each surface perpendicular to the coordinate axis; applying normal displacement on the surface perpendicular to x_i; and restraining normal displacement of each surface perpendicular to $x_j (j \neq i)$. For ideal periodically filled composites with the given boundary conditions, the macro effective strain and stress field are presented as

$$\langle \varepsilon_i^i \rangle = \frac{\Delta l}{d_i},\ \varepsilon_j^i = 0 \quad \text{(Eq 2)}$$

$$\langle \sigma_i^i \rangle = \frac{1}{A_i} \int_{A_i} \sigma(x_i) dA, \quad \left\langle \sigma_j^i \right\rangle = \frac{1}{A_j} \int_{A_j} \sigma_j^i dA \quad \text{(Eq 3)}$$

where the superscript is the load direction, and A_i is any cross-sectional area perpendicular to x_i.

MHS periodically filled composite is a typical kind of orthotropic material. Generalized Hooke's law of orthotropic material is

$$\{\sigma\} = [D]\{\varepsilon\} \quad \text{(Eq 4)}$$

where $[D]$ is stiffness matrix, that is

$$[D] = \begin{bmatrix} C_{11} & C_{12} & C_{13} & 0 & 0 & 0 \\ & C_{22} & C_{23} & 0 & 0 & 0 \\ & & C_{33} & 0 & 0 & 0 \\ & & & G_{23} & 0 & 0 \\ & & & & G_{31} & 0 \\ & & & & & G_{12} \end{bmatrix} \quad \text{(Eq 5)}$$

where G is the shear modulus.

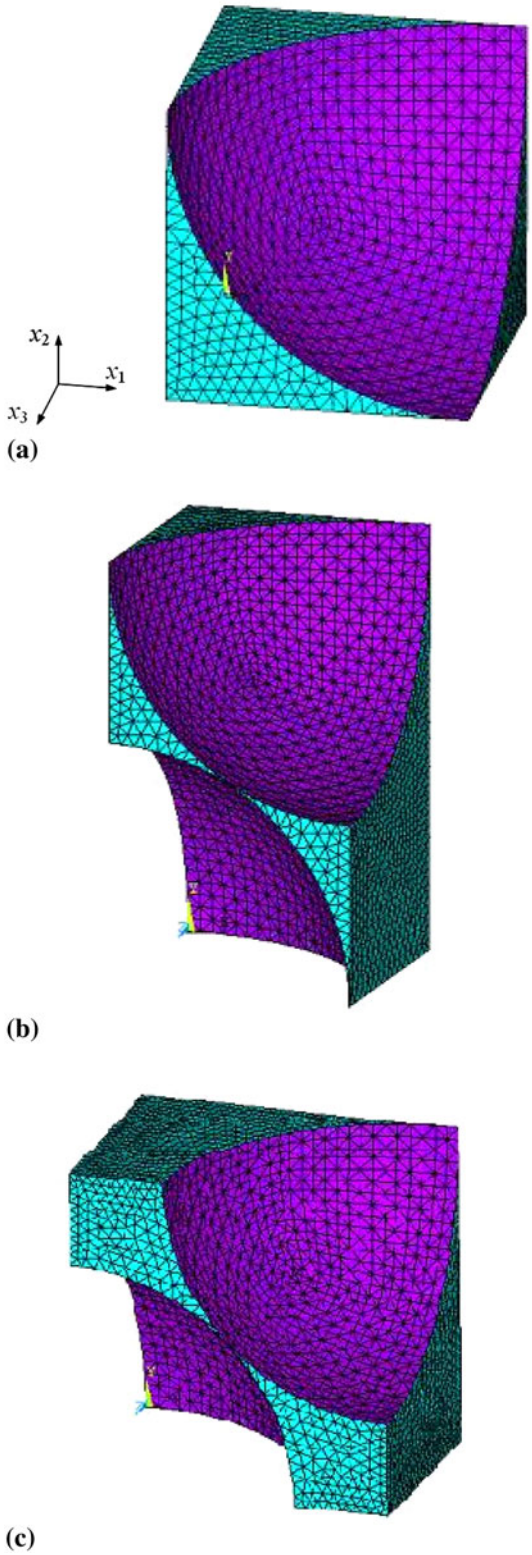

Fig. 2 The unit cells and meshing. (a) SC, (b) FHC and (c) CSC

Under the three-dimensional loading, the corresponding resultant forces of cross section perpendicular to loading direction are obtained from finite element analyses. Then, the stress and strain can be obtained according to Eq 2 and 3. Based on Eq 4 and 5 and boundary conditions, the effective macro stress and stiffness coefficient can be calculated.

Flexibility matrix $[S]$ is the inverse of matrix $[D]$, that is

$$\{\varepsilon\} = [S]\{\sigma\} \quad \text{(Eq 6)}$$

where, $S_{11} = (C_{22}C_{33} - C_{23}^2)/C$; $S_{22} = (C_{11}C_{33} - C_{13}^2)/C$; $S_{33} = (C_{22}C_{11} - C_{12}^2)/C$; $S_{23} = (C_{21}C_{31} - C_{23}C_{11})/C$; $S_{31} = (C_{32}C_{12} - C_{21}C_{22})/C$; $S_{12} = (C_{13}C_{23} - C_{12}C_{33})/C$; $C = C_{11}C_{22}C_{33} - C_{11}C_{23}^2 - C_{22}C_{13}^2 - C_{33}C_{12}^2 + 2C_{12}C_{23}C_{13}$.

Then, some of the elastic constants can be calculated by following equations:

$$S_{11} = \frac{1}{E_1}, \quad S_{22} = \frac{1}{E_2}, \quad S_{33} = \frac{1}{E_3} \quad \text{(Eq 7)}$$

$$S_{12} = -\frac{\mu_{12}}{E_2}, \quad S_{31} = -\frac{\mu_{31}}{E_1}, \quad S_{23} = -\frac{\mu_{23}}{E_3} \quad \text{(Eq 8)}$$

3. Results and Discussion

As shown in Table 2, the data of effective elastic modulus changes with the wall thickness. From this table, it can be seen that the effective elastic modulus in each direction for the three packing types increases with the increase in wall thickness. It is also found that the effective elastic modulus of composite for the three packing types is larger than that of MHSS in the literature (Ref 7, 16), although the elastic modulus of constituent material of MHS in this article is lower than that in the literature. This shows that the epoxy in the composite plays an important role on the mechanical properties. The modulus of composite for SC packing type in each direction has the same values. That is to say, the composite for SC packing type can be considered as orthogonal isotropic material. The composite for SC packing type is similar to the syntactic MHSS, indicated in the literature (Ref 7). The results obtained in this article are slightly less than the results in the literature. The main reasons for this are the smaller data of material properties for MHS and the epoxy adopted.

Figure 3 shows a comparison of elastic moduli of composites in the direction of x_1 for the three packing types. From Fig. 3, it is seen that the elastic moduli of composites for the three packing types increase logarithmically with the increase in wall thickness. The effect of changing MHS packing type on effective elastic modulus of composites is also found. However, the effect decreases with the increase in wall thickness. The maximum difference is about 26% when the MHS wall thickness is 0.1 mm, but the three curves merge, when the wall thickness is about 0.85 mm.

In addition, it is found that the elastic modulus for SC is larger than that for FHC and CSC. However, the elastic modulus for SC is the minimum as found in other studies (Ref 3, 16). The MHS/EP composite contains two kinds of materials, i.e., MHS and epoxy. Their interaction is another reason why there is a difference of modulus between MHS and MHS/EP. In addition, the elastic modulus of epoxy is larger than that of hollow sphere. The volume ratio of MHS for SC is smaller than that for FHC, and so the elastic modulus for SC is larger because of its containing more epoxy. Although, the CSC packing type is the 45° rotation of SC packing type around the x_3 axis, the modulus is larger than that of SC. This suggested that the elastic modulus changes along with the change of loading direction. However, a conclusion of quasi-isotropic was obtained by Fiedler and Öchsner (Ref 7). This reason for the difference is the different morphologies between composites for SC packing type and syntactic MHSS.

Figure 4 shows the curves of effective elastic modulus in each direction changed with wall thickness for FHC and CSC packing types. Figure 4(a) and (b) show the same change laws. The elastic moduli of composites for FHC and CSC packing types in the directions of x_1 and x_2 are approximately coincident, but there are more differences with it in the direction of x_3. The difference decreases with the increase of wall thickness. Thus, it can be suggested that the composites for FHC and CSC packing types are orthotropic, but not obvious, and they can be considered as orthogonal isotropic in relation to their linear-elastic behavior when the wall thickness is about 0.85 mm. At this time, the value t/R of shell is about 0.074.

In this article, the diameter of MHS shell is 23 mm. If the value of t/R equals 0.05, then it is considered as the dividing line between the thin-walled shell and the medium-thickness shell, and the critical thickness of shell is 0.575. From Fig. 4, the elastic constants in three directions have a little difference when the t/R of shell is 0.05, and it decreases with the increase in t/R. Therefore, it can be concluded that the value t/R has an effect on the effective behavior of composites. From Fig. 3 and 4, it is found that all the values of elastic moduli are very close when the value of t/R is 0.074. It is suggested that the packing

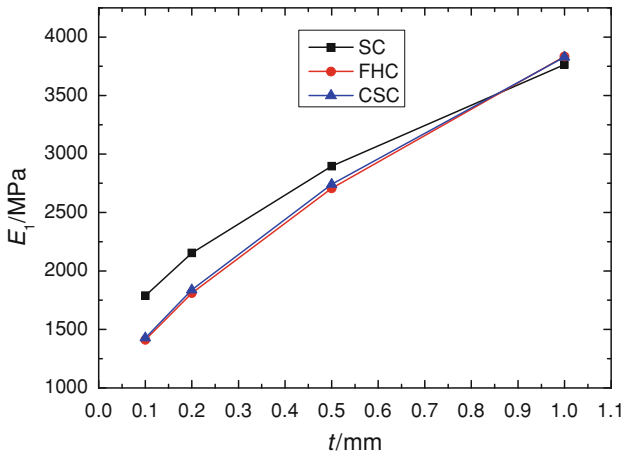

Fig. 3 The effective elastic modulus in x_1 direction

Table 2 The effective elastic modulus of the three models

Packing types	SC				FHC				CSC			
t, mm	0.1	0.2	0.5	1.0	0.1	0.2	0.5	1.0	0.1	0.2	0.5	1.0
E_1, MPa	1778	2153	2896	3764	1410	1810	2707	3834	1427	1838	2740	3828
E_2, MPa	1778	2153	2896	3764	1409	1809	2706	3833	1427	1838	2740	3828
E_3, MPa	1778	2153	2896	3764	1511	1945	2801	3786	1797	2160	2899	3763

type has no effect on the mechanical behavior when the value of t/R equals 0.074. The shell is with a medium-thickness wall at this time.

Table 3 shows the effective Poisson's ratios changed with wall thickness of the composites for the three packing types. It is found that the effective Poisson's ratios of the composite are the same in three directions for SC packing type, but they have a large difference in the three directions for FHC and CSC packing types. Their changes along with the increase of wall thickness are different too.

Figure 5 shows the curves of Poisson's ratios in each direction changed with wall thickness of each packing type. From Fig. 5(a), the Poisson's ratios of composite in three directions for FHC packing type are different. Their change trends along with the increase of wall thickness are different too. The varying trends of μ_{23} are approximately the same as that for SC packing type. However, μ_{12} decreases with the increase of the wall thickness. The variation curve of μ_{31} is located between them. These phenomena further verify its orthogonal anisotropic property. However, the three curves also merge when the wall thickness is about 0.85 mm. The value of t/R equals 0.074 at this time. It is also suggested that the value of t/R has an effect on the effective behavior of composites. The Poisson's ratios for CSC packing type have the same varying trends, as can be seen in Fig. 5(b). Based on the curves of effective modulus, it can be concluded that the composites for FHC and CSC packing types have an orthogonal isotropic property when the value of t/R is 0.074.

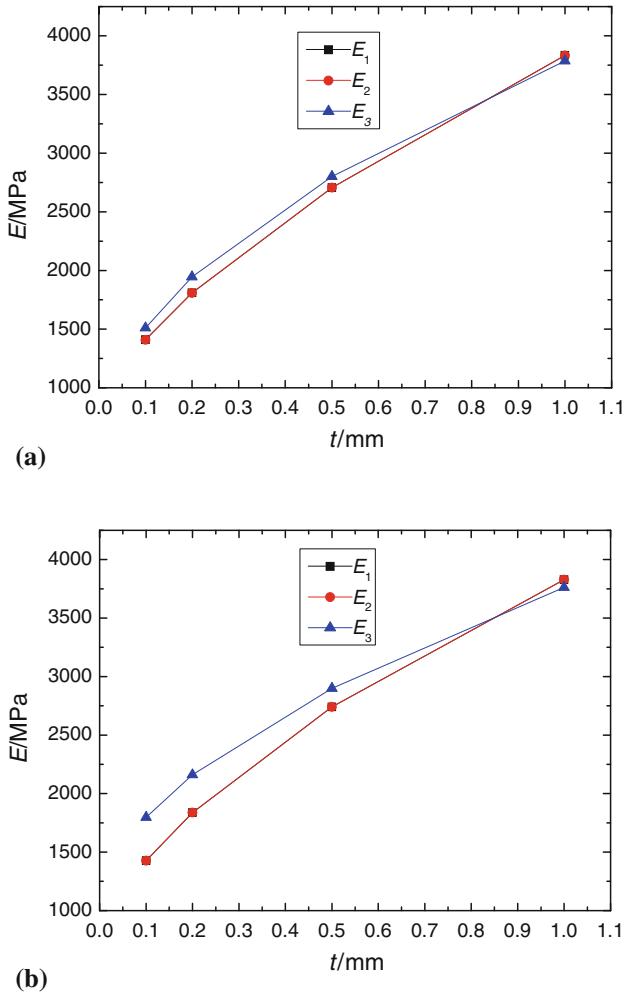

Fig. 4 The effective elastic modulus of composites for (a) FHC and (b) CSC

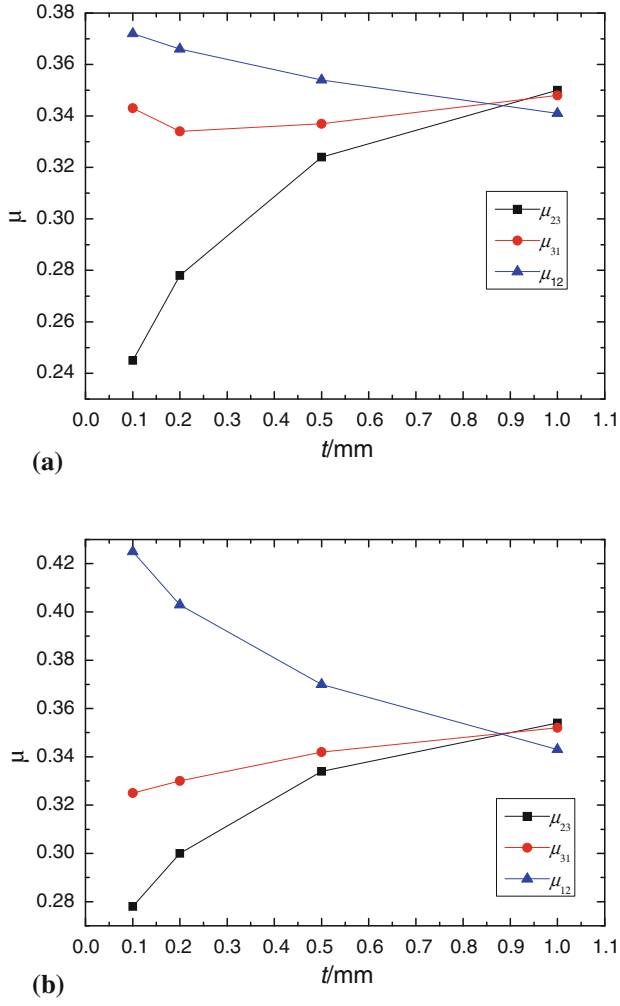

Fig. 5 The curves between Poisson's ratios and wall thickness. (a) FHC and (b) CSC

Table 3 The effective Poisson's ratios for the three type composites

Packing types	SC				FHC				CSC			
t, mm	0.1	0.2	0.5	1.0	0.1	0.2	0.5	1.0	0.1	0.2	0.5	1.0
μ_{12}	0.277	0.299	0.334	0.353	0.372	0.366	0.354	0.341	0.425	0.403	0.370	0.343
μ_{23}	0.277	0.299	0.334	0.353	0.245	0.278	0.324	0.350	0.277	0.300	0.334	0.354
μ_{31}	0.277	0.299	0.334	0.353	0.343	0.334	0.337	0.347	0.325	0.330	0.342	0.351

From Fig. 3 to 5, it can be concluded that there is an effect of the packing type of MHS on the effective elastic modulus and Poisson's ratio of composite when the shell is thin-walled ($t/R < 0.05$). However, the effect on them is minor when the shell is medium-thickness wall ($t/R > 0.05$), especially the value t/R of 0.074.

4. Conclusion

The composite for SC packing type is orthogonal isotropic material. However, the composites for FHC and CSC packing types are orthotropic material, but the orthotropic properties decrease with the increase of wall thickness of MHS. They present orthogonal isotropic properties when the wall thickness is about 0.85 mm; at this time, the value of t/R is about 0.074. Based on the analysis above, it can be concluded that the composites for FHC and CSC packing types should be considered as orthotropic material in relation to their linear-elastic behavior when the shell is thin-walled ($t/R < 0.05$). However, they can be considered as orthogonal isotropic materials when the shell is medium-thickness wall ($t/R > 0.05$). Moreover, it can be inferred that the packing type of MHS is not important for the studies on the linear-elastic behavior when the shell is with a medium-thickness wall, especially the value of 0.074 for the ratio t/R.

Acknowledgments

This study is funded by the Hebei Natural Science Foundation (E2011203230) and the Hebei Institution of Higher Education scientific research plan (2010166).

References

1. L.J. Gibson and M.F. Ashby, *Cellular Solids: Structure and Properties*, Cambridge University Press, Cambridge, 1997
2. T.J. Lu, D.P. He, C.Q. Chen, C.Y. Zhao, D.N. Fang, and X.L. Wang, The Multi-Functionality of Ultra-Light Porous Metals and Their Applications, *Adv. Mech.*, 2006, **36**(4), p 517–535
3. W.S. Sanders and L.J. Gibson, Mechanics of BCC and FCC Hollow-Sphere Foams, *Mater. Sci. Eng. A*, 2003, **352**(1–2), p 150–161
4. T.J. Lim, B. Smith, and D.L. Mcdowell, Behavior of a Random Hollow Sphere Metal Foam, *Acta Mater.*, 2002, **50**(11), p 2867–2879
5. S. Gasser, F. Paun, A. Cayzeele, and Y. Brechet, Uniaxial Tensile Elastic Properties of a Regular Stacking of Brazed Hollow Spheres, *Scripta Mater.*, 2003, **48**(12), p 1617–1623
6. S. Gasser, F. Paun, and Y. Bréchet, Finite Elements Computation for the Elastic Properties of a Regular Stacking of Hollow Spheres, *Mater. Sci. Eng. A*, 2004, **379**(1–2), p 240–244
7. T. Fiedler and A. Öchsner, On the Anisotropy of Adhesively Bonded Metallic Hollow Sphere Structures, *Scripta Mater.*, 2008, **58**(8), p 695–698
8. T. Fiedler, E. Solórzano, and A. Öchsner, Numerical and Experimental Analysis of the Thermal Conductivity of Metallic Hollow Sphere Structures, *Mater. Lett.*, 2008, **62**(8–9), p 1204–1207
9. T. Fiedler, R. Löffler, T. Bernthaler, R. Winkler, and A. Öchsner, Numerical Analyses of the Thermal Conductivity of Random Hollow Sphere Structures, *Mater. Lett.*, 2009, **63**(13–14), p 1125–1127
10. E. Solórzano, M.A. Rodríguez-Perez, and J.A. de Saja, Thermal Conductivity of Metallic Hollow Sphere Structures: An Experimental, Analytical and Comparative Study, *Mater. Lett.*, 2009, **63**(13–14), p 1128–1130
11. F. Feyel and V. Marcadon, Modelling of the Compression Behaviour of Metallic Hollow-Sphere Structures: About the Influence of Their Architecture and Their Constitutive Material's Equations, *Comput. Mater. Sci.*, 2009, **47**(2), p 599–610
12. P. Lhuissier, A. Fallet, L. Salvo, and Y. Brechet, Quasistatic Mechanical Behaviour of Stainless Steel Hollow Sphere Foam: Macroscopic Properties and Damage Mechanisms Followed by X-Ray Tomography, *Mater. Lett.*, 2009, **63**(13–14), p 1113–1116
13. O. Friedl, C. Motz, H. Peterlik, S. Puchegger, H. Reger, and R. Pippan, Experimental Investigation of Mechanical Properties of Metallic Hollow Sphere Structures, *Metall. Mater. Trans. B*, 2008, **39**, p 135–146
14. H.H. Ruan, Z.Y. Gao, and T.X. Yu, Crushing of Thin-Walled Spheres and Sphere Arrays, *Int. J. Mech. Sci.*, 2006, **48**(2), p 117–133
15. D. Karagiozova, T.X. Yu, and Z.Y. Gao, Modelling of MHS Cellular Solid in Large Strains, *Int. J. Mech. Sci.*, 2006, **48**(11), p 1273–1286
16. Z.Y. Gao, T.X. Yu, and D. Karagiozova, Finite Element Simulations on the Mechanical Properties of MHS Materials, *Acta Mech. Sin.*, 2007, **23**(1), p 65–75
17. X.L. Dong, Z.Y. Gao, and T.X. Yu, Dynamic Crushing of Thin-Walled Spheres: An Experimental Study, *Int. J. Impact Eng.*, 2008, **35**(8), p 717–726
18. A. Tasdemirci, C. Ergonenc, and M. Guden, Split Hopkinson Pressure Bar Multiple Reloading and Modeling of a 316 L Stainless Steel Metallic Hollow Sphere Structure, *Int. J. Impact Eng.*, 2010, **37**(3), p 250–259
19. C. Motz, O. Friedl, and R. Pippan, Fatigue Crack Propagation in Cellular Metals, *Int. J. Fatigue*, 2005, **27**(10–12), p 1571–1581
20. O. Caty, E. Maire, T. Douillard, P. Bertino, R. Dejaeger, and R. Bouchet, Experimental Determination of the Macroscopic Fatigue Properties of Metal Hollow Sphere Structures, *Mater. Lett.*, 2009, **63**(13–14), p 1131–1134
21. C. Augustin and W. Hungerbach, Production of Hollow Spheres (HS) and Hollow Sphere Structures (HSS), *Mater. Lett.*, 2009, **63**, p 1109–1112